Evidence for the Predominance of Subsurface Defects on Reduced Anatase $TiO_2(101)$

Yunbin He,[1] Olga Dulub,[1] Hongzhi Cheng,[2] Annabella Selloni,[2] and Ulrike Diebold[1,*]

[1]*Department of Physics, Tulane University, New Orleans, Louisiana 70118, USA*

[2]*Department of Chemistry, Princeton University, Princeton, New Jersey 08544, USA*

(Received 15 October 2008; revised manuscript received 12 January 2009; published 13 March 2009)

Scanning tunneling microscopy (STM) images taken on a freshly cleaved anatase $TiO_2(101)$ sample show an almost perfect surface with very few subsurface impurities and adsorbates. Surface oxygen vacancies are not typically present but can be induced by electron bombardment. In contrast, a reduced anatase (101) crystal shows isolated as well as ordered intrinsic subsurface defects in STM, consistent with density functional theory (DFT) calculations which predict that O vacancies (V_O's) at subsurface and bulk sites are significantly more stable than on the surface.

DOI: 10.1103/PhysRevLett.102.106105 PACS numbers: 68.47.Gh, 68.35.Dv, 68.37.Ef

Titanium dioxide, TiO_2, finds applications in a wide range of technological fields. This reducible metal oxide accommodates a large degree of substoichiometry. The resulting intrinsic defects can strongly affect the physicochemical properties of this material. Native defects can also form to compensate the charges of foreign dopants [1]. Doping with extrinsic impurities is particularly promising to functionalize TiO_2 as, e.g., a visible-light photocatalyst [2] or dilute magnetic semiconductor [1,3]. The importance of defects has motivated extensive studies of their structure, both in the bulk [4] and on the surface [5]. In particular, STM studies have established with intricate detail the role of surface O vacancies in surface chemistry on rutile $TiO_2(110)$ [6,7]. The TiO_2 polymorph anatase has great importance in technical applications and fundamental nanoscience but, in contrast to the vast literature on rutile and many theoretical studies on anatase [8–12], very few experimental studies on well-characterized anatase surfaces are available.

STM [13] and adsorption [14] experiments indicated that a vacuum-prepared anatase (101) surface contains far fewer V_O's than those typically present on a rutile (110) surface [5]. However, spectroscopy studies found that, under comparable preparation conditions, anatase (101) potentially accommodates more defects than rutile (110) in the surface region [15]. Our combined experimental and DFT study provides direct evidence of subsurface defects at anatase (101), thus solving the apparent contradiction between these previous experimental findings [13–15]. STM shows that these defects have a strong tendency to form linear chains, even at low concentrations. This is explained by a model, where a subsurface V_O triggers the formation of Frenkel pairs (Ti interstitials (Ti_i) and Ti vacancies (V_{Ti})). Given the key role of defects in defining the surface properties of oxides [5,16], these findings should further our understanding of this important material.

The DFT calculations were carried out within the generalized gradient approximation [17]. The plot in Fig. 1(a) reports the V_O formation energy for various surface and subsurface sites within a slab containing 6 TiO_2 layers (216 atoms); a more detailed account of this study is presented in Ref. [12]. On the surface, the removal of a

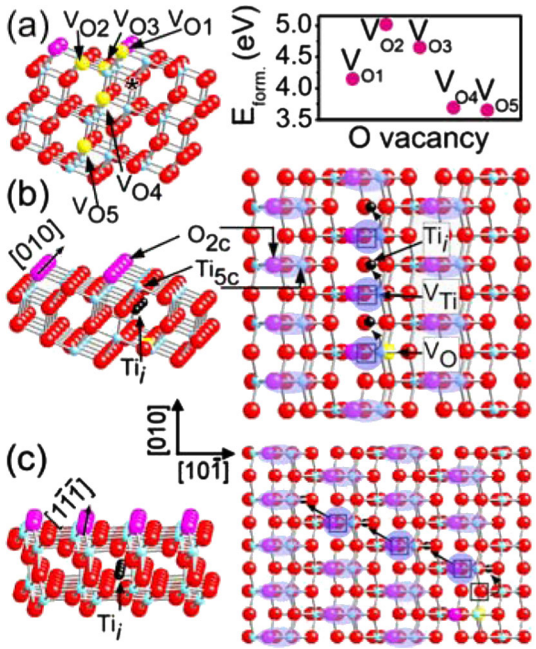

FIG. 1 (color online). Models of anatase $TiO_2(101)$ in side (left) and top (right) view (red balls: O; light blue balls: Ti). The purple shading indicates the contrast of atomically-resolved STM images, ovals extending across undercoordinated surface O_{2c} and Ti_{5c} on undisturbed surface and circles above subsurface defects. (a) Various on- and subsurface O vacancies (left) and their corresponding formation energies (right); only part of the six-layer-thick slab used for the calculations is shown. (b), (c) Illustration of formation of ordered subsurface defects invoking Frenkel hops. Formation of a subsurface O vacancy (yellow) initiates the migration of a neighboring Ti atom to an interstitial site (Ti_i, black), leaving behind a Ti vacancy (V_{Ti}, black square). This process is repeated along open channels parallel to the crystallographic (b) [010] and (c) [1$\bar{1}$ $\bar{1}$] directions.

twofold-coordinated oxygen atom (O_{2c}), V_{O1}, is the energetically most favorable V_O defect. Among subsurface sites, the site directly below the surface O_{2c} (marked with an asterisk) is unstable: if a vacancy is created at that site, the O_{2c} atom just above it moves spontaneously to fill the vacancy, leaving a surface V_{O1} defect. Most importantly, the formation energies of the subsurface V_{O4} and V_{O5} defects in Fig. 1(a) are *lower* than the energy cost to form V_{O1}, or other surface O vacancies. Estimations of diffusion pathways [12] show a relatively low (~0.7 eV) barrier for diffusion of V_O's from a surface to a subsurface site, and a significantly higher barrier for the reverse process. In contrast, calculations with the same theoretical setup on rutile (110) show that O vacancies at the bridging oxygen sites are substantially more favorable than subsurface defects [12].

The experiments were performed in ultrahigh vacuum (UHV). The sample was cleaned *in situ* by cycles of Ar^+ ion sputtering and annealing to 600 °C. STM was performed in the constant-current mode; empty states were typically imaged. Both anatase samples were natural mineral crystals, originally orange-clear in color, and became darker blue with repeated sputtering and annealing cycles.

The first sample was cleaved *ex situ*. After a few cleaning cycles, low energy electron diffraction (LEED) shows a sharp (1×1) pattern. As seen in Fig. 2(a), the freshly cleaved surface is rather pristine. The terraces have the typical trapezoidal shape described earlier [13]. The oval-shaped, atomic-sized features extend over both surface Ti_{5c} and O_{2c} atoms (see also Fig. 1) arranged in rows along the [010] direction. A few black spots [arrow in Fig. 2(b)] are situated on top of an oval. Their density amounts to ~0.5% of a monolayer (ML), where one ML is defined as the number of Ti_{5c}-O_{2c} ovals on a perfect (101) surface. We attribute these to adsorbates, probably water. Some nm-wide, brighter features are visible as well. The one circled in Fig. 2(b) shows a corrugation of 0.57 Å that extends over 6 lattice units in the [010] direction, although the apparent height depends on the tunneling conditions. This behavior is reminiscent of charged dopants in Si and compound semiconductors [18]; the large-scale corrugation is induced by the screened Coulomb potential, which results in local band bending. We attribute the nm-wide features to extrinsic impurities, also because their density decreased in repeated sputtering and annealing cycles and they vanished eventually. From STM we estimate an impurity concentration of 0.05 at% within the first few layers. This is well below the detection limit for x-ray photoelectron spectroscopy (XPS); indeed, no contaminants were found in extensive XPS scans.

In order to establish how surface V_O's appear in STM, we irradiated the sample with electrons. Electron bombardment of TiO_2 induces the desorption of surface oxygen and can be used to create V_O's [7,19]. Figure 2(c) shows the surface after irradiation with 300 eV electrons at a dose of 6.9×10^{16} e^-/cm^2. Extra-bright spots with a density of

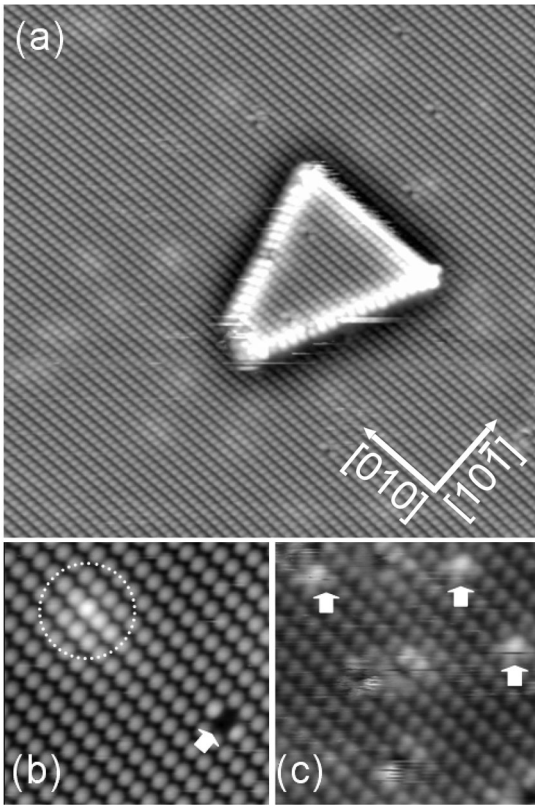

FIG. 2. STM images from a freshly cleaved anatase (101) surface. (a) Large-scale overview (300×300 Å^2; $V_{sample} = +1.3$ V, $I_{tunnel} = 1.9$ nA). (b) High-resolution image (70×70 Å^2; +1.6 V, 1.6 nA). The dotted circle indicates a subsurface impurity, the arrow an adsorbate, probably water. (c) After irradiation with 300 eV electrons (70×70 Å^2; +1.5 V, 2 nA), which creates surface O vacancies (marked with arrows).

~1.8% appear [arrows in Fig. 2(c)]; their STM contrast agrees with calculations of V_O's on anatase (101) [10]. These vacancies do not "survive" long in the residual gas; they become covered with adsorbates from the residual gas, probably water [11], and move under the STM tip, so that the surface becomes more difficult to image.

The second sample was a cut [along (101)] and polished mineral specimen that was used in our laboratory for several years. Originally, it showed a very similar appearance as the freshly cleaved, pristine sample, and XPS indicated the Ti^{4+} peak typical for a stoichiometric surface [Fig. 3(a)], again, with no trace of extrinsic impurities over wide scans. This sample was subjected to >150 sputter and annealing cycles over the course of many experiments. While LEED still shows a high-quality (1×1) pattern, the XPS Ti $2p$ line indicates a reduced surface [cf. Fig. 3(b)]. The intensity ratio of the Ti^{3+}:Ti^{4+} $2p_{3/2}$ peaks amounts to ~20%, demonstrating a marked substoichiometry within the probing depth of XPS.

Figure 4(a) shows a wide-scale STM image taken on this reduced anatase (101) sample. It exhibits black spots, which often form short chains along [010], [11$\bar{1}$], and

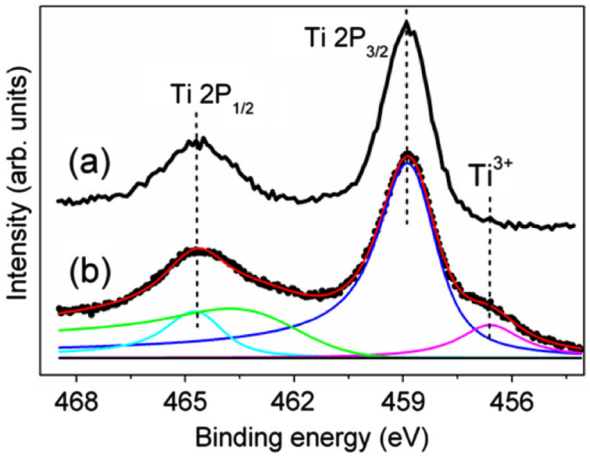

FIG. 3 (color online). Comparison of XPS Ti $2p$ lines of a freshly cleaved (a) and a reduced (b) anatase (101) surface.

$[1\bar{1}\,\bar{1}]$ directions [Fig. 4(a) inset]. The dark spots are different from both the adsorbates [Fig. 2(b)] and surface O vacancies [Fig. 2(c)]. Similar to the extrinsic impurities shown in Fig. 2(b) above, their appearance depends sensitively on the STM tunneling parameters [20]. As mentioned above, atomically-resolved STM anatase (101) typically shows bright "ovals." On the reduced sample, under tunneling conditions that keep the tip further away from the surface, some of these ovals become small, round spots. The half ovals have different brightness, as indicated with circles of different color in Fig. 4(b). Some of the half ovals appear isolated, but most of them reside in short chains along [010], $[11\bar{1}]$, or $[1\bar{1}\,\bar{1}]$ directions. Often, full ovals next to the half ovals are somewhat brighter and more elongated [marked with short lines in Fig. 4(b)]. Counting the number of defects classified as half-ovals (circles) and extra-bright full ovals (short lines) in Fig. 4(b) and similar images yields a density of $\sim$0.16 ML. In addition to these full and half-ovals, STM shows a small number of extra-bright features [0.02–0.03 ML, marked with dashed ellipses in Fig. 4(b)]. Their appearance is independent of the tunneling conditions applied. They occasionally change positions between consecutive scans. From control experiments, where water was dosed on anatase (101) at low temperatures, we tentatively assign them as water molecules, possibly adsorbed at defect sites. The features marked with black squares in Fig. 4(b) might be surface impurities, which, because of their small concentration ($<$0.01 ML), remain currently unidentified.

To summarize, (i) we observe defects on clean, reduced anatase (101) that are not visible on more pristine, stoichiometric surfaces; (ii) their density increases with bulk reduction induced by repeated sputter and annealing cycles; (iii) these defects are clearly different from surface V_O's produced by e^- bombardment; (iv) they do not become covered with adsorbates upon prolonged exposure to the residual gas in UHV chambers; i.e., are relatively inert;

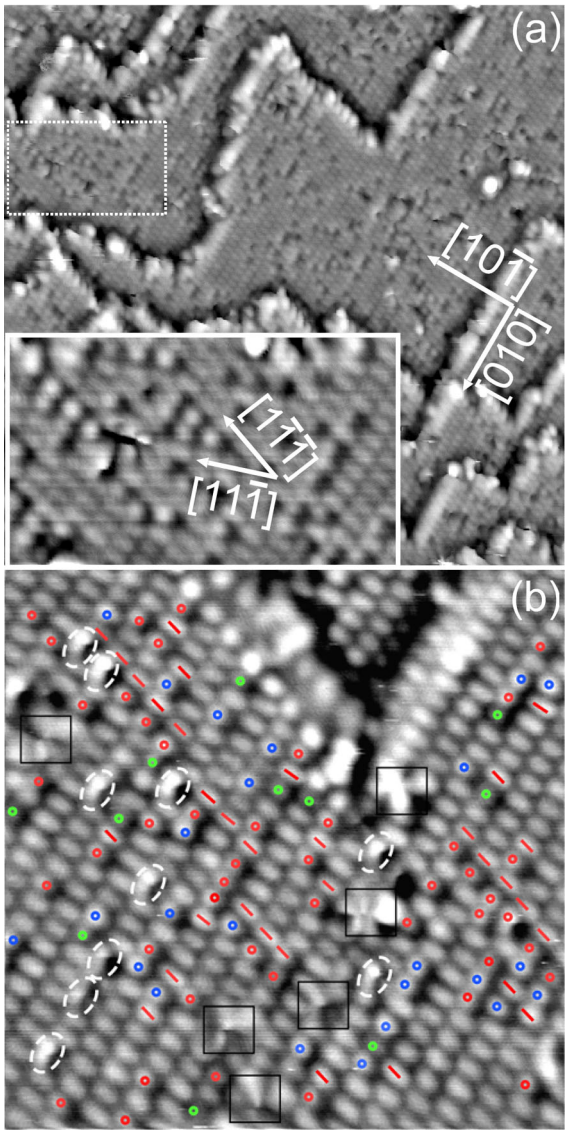

FIG. 4 (color online). STM images of the reduced anatase (101) surface. (a) Large-scale overview (300×300 Å^2; +1.2 V, 0.9 nA). The dark spots are attributed to subsurface defects. As shown in the inset, they exhibit tendency to line up along [010], $[1\bar{1}\,\bar{1}]$, and $[11\bar{1}]$ directions. (b) High-resolution image (100×100 Å^2; +1.2 V, 0.1 nA) with subsurface defects. Marked with colored circles are half ovals that are darker (green), same brightness (red), or brighter (blue) than regular ovals; red dashes mark extra-bright ovals. Features marked by dotted ellipses and black squares are tentatively assigned to adsorbates and surface impurities, respectively.

and (v) their contrast in STM is subtle and bias or current dependent, pointing towards changes in the surface electronic, rather than geometric structure. These observations, combined with our DFT results, lead us to conclude that intrinsic defects on anatase (101) are predominantly located subsurface. This result in itself is significant; while it is well-known that surface O vacancies have a vast influence on surface chemistry, it appears that, for this important material, mostly subsurface defects have to be con-

sidered. Before discussing potential implications, however, we turn to an analysis of the defect structures observed in STM. Since there are a much larger number of defect configurations in the bulk than on the surface this analysis must necessarily remain speculative, but important insights can nevertheless be gained.

First, note that substoichiometry in TiO_2 can be introduced through both O vacancies and excess Ti (present in the form of interstitials, Ti_i). The relative abundance of these intrinsic defects in dependence of external parameters (p, T, impurities) has been the subject of long debate [4], and besides well-acknowledged surface V_O's, interstitials may also play a role on the rutile (110) surface [21]. Subsurface O vacancies alone cannot account for all defects seen in STM for the reduced anatase (101). In particular, the linear ordering is hard to reconcile based solely on V_O's, as removal of whole chains of O atoms would result in a large number of unsaturated bonds within the crystal. In order to rationalize our observations, we resort to the knowledge gained from extensive studies on rutile [4]. Bulk defects in reduced rutile tend to form arrays, even when present in small densities. For highly reduced samples the ordering results in crystallographic shear planes (CSP's) that order into Magnéli phases [4]. Bursill and Blanchin [4] proposed a structural model that provides a logical route from small defect aggregates to the CSP's. This model is based on the formation of Frenkel (neighboring V_{Ti}-Ti_i) pairs. We adopt this idea to explain the linear chains of half ovals in our STM images: Suppose a V_O, created by annealing, migrates to a subsurface site [the yellow atom in Figs. 1(b) and 1(c)]. In Ref. [4] it was argued that even an isolated V_O results in the formation of a ''reconstructed defect'', where a Ti neighbor atom migrates to the next interstitial site. According to ref. the most favorable site for a Ti_i in anatase is at the side of the open channels that run along the [010] direction [8] [see side view in Fig. 1(b); black balls mark Ti_i]. Once such a Ti_i is formed, the neighboring Ti atom is destabilized and pushed towards the next interstitial position (via a ''Frenkel hop''), resulting in lines of V_{Ti} and Ti_i sites [black squares and black balls, respectively, in Fig. 1(b)]. Such linear arrays will form along open channels that allow for a facile motion of Ti_i, along [010] [Fig. 1(b)] and $[1\bar{1}\,\bar{1}]$ or $[11\bar{1}]$ [Fig. 1(c)]. The V_{Ti} resides underneath an O_{2c}-Ti_{5c} unit [top views in Fig. 1(b) and 1(c)]. The screened Coulomb potential induced by a negative charge in an n-type semiconductor (such as reduced anatase) leads to a depression in empty-states STM images [18]. We thus hypothesize that negatively charged V_{Ti}'s induces a depression, canceling the contrast from the surface Ti_{5c} atoms above and creating the ''half ovals'' observed in STM images.

Our finding, namely, that defects on anatase reside predominantly subsurface and have a tendency to form linear arrays—best explained by Frenkel pairs—has broad implications for understanding the materials properties of TiO_2 anatase. Subsurface defects are less reactive than surface oxygen vacancies. In TiO_2-based photocatalysis [22] defects act as trap sites for photo-excited charge carriers. If they are located on the surface, they are quenched by adsorption of molecules from the ambient. When located just beneath the top surface layer, they could survive and steer photo-excited charge carriers to near-surface regions. Potentially the propensity of anatase to form subsurface defects contributes to its superior photocatalytic properties. Intrinsic defects are thought to be instrumental for the ferromagnetic properties of doped TiO_2 [1]. While O vacancies are usually considered, our results show that the strong tendency to Ti vacancies and interstitials should be taken into account as well.

We thank Shao-chun Li for helpful discussions. Support from the U.S. Department of Energy (grant DE-FG02-05ER15702) and National Science Foundation (CHE-0715576) is acknowledged.

*Corresponding author.
diebold@tulane.edu

[1] S. A. Chambers, Surf. Sci. Rep. **61**, 345 (2006).
[2] R. Asahi *et al.*, Science **293**, 269 (2001).
[3] Y. Matsumoto *et al.*, Science **291**, 854 (2001).
[4] M. G. Blanchin, Key Eng. Mater. **155–156**, 359 (1998); L. A. Bursill and M. G. Blanchin, J. Phys. Lett. **44**, 165 (1983); J. Solid State Chem. **51**, 321 (1984).
[5] U. Diebold, Surf. Sci. Rep. **48**, 53 (2003).
[6] O. Bikondoa *et al.*, Nature Mater. **5**, 189 (2006); R. Schaub *et al.*, Phys. Rev. Lett. **87**, 266104 (2001); Z. Zhang *et al.*, J. Phys. Chem. B **110**, 21840 (2006).
[7] C. L. Pang *et al.*, Nanotechnology **17**, 5397 (2006).
[8] S. Na-Phattalung *et al.*, Phys. Rev. B **73**, 125205 (2006).
[9] J. He *et al.*, Acta Mater. **55**, 4325 (2007).
[10] E. Finazzi *et al.*, J. Phys. Chem. C **111**, 9275 (2007).
[11] A. Tilocca and A. Selloni, J. Phys. Chem. B **108**, 4743 (2004).
[12] H. Cheng and A. Selloni, Phys. Rev. B (to be published).
[13] W. Hebenstreit *et al.*, Phys. Rev. B **62**, R16 334 (2000); X.-Q. Gong *et al.*, Nature Mater. **5**, 665 (2006).
[14] G. S. Herman *et al.*, J. Phys. Chem. B **107**, 2788 (2003).
[15] A. G. Thomas *et al.*, Phys. Rev. B **75**, 035105 (2007).
[16] F. Esch *et al.*, Science **309**, 752 (2005).
[17] J. P. Perdew, K. Burke, and M. Ernzerhof, Phys. Rev. Lett. **77**, 3865 (1996); S. Baroni *et al.*, http://www.democritos.it.
[18] P. Ebert, Surf. Sci. Rep. **33**, 121 (1999).
[19] O. Dulub *et al.*, Science **317**, 1052 (2007).
[20] See EPAPS Document No. E-PRLTAO-102-006913 for STM images of reduced anatase (101) under varying tunneling conditions. For more information on EPAPS, see http://www.aip.org/pubservs/epaps.html.
[21] S. Wendt *et al.*, Science **320**, 1755 (2008).
[22] A. L. Linsebigler, G. Lu, and J. T. Yates, Chem. Rev. **95**, 735 (1995).